

SOLID STATE LASERS FROM AN EFFICIENCY PERSPECTIVE

Norman P. Barnes
NASA Langley Research Center
Hampton, VA 23681 U.S.A.

Abstract: Solid state lasers have remained a vibrant area of research because several major innovations expanded their capability. Major innovations are presented with emphasis focused on the laser efficiency. A product of efficiencies approach is developed and applied to describe laser performance. Efficiency factors are presented in closed form where practical and energy transfer effects are included where needed. In turn, efficiency factors are used to estimate threshold and slope efficiency, allowing a facile estimate of performance. Spectroscopic, thermal, and mechanical data are provided for common solid state laser materials.

Index terms: Solid state lasers, laser efficiency, diode pumped solid state lasers, laser modeling

Introduction:

Solid state lasers remain a vibrant area because of several innovations in technology and because they have capabilities available with no other type of laser. These innovations have opened up fruitful new areas for solid state laser research. Directly below, 4 major innovations appear with other innovations scattered throughout the text. Some important solid state laser capabilities result from their ability to store energy. Efficient energy storage for millisecond time intervals is unique to solid state lasers. Energy storage permits solid state lasers to serve as optical integrators. Low brightness optical pumps can be optically integrated and laser energy delivered in a high peak power and high brightness laser beam. This capability of solid state lasers is a prime reason for their utility.

The first innovation was the invention of the laser itself, a solid state Cr:Al₂O₃ laser, [1]. Although this laser had a low efficiency, its discovery stirred imaginations. Uses for lasers, such as laser induced nuclear fusion and laser weaponry were conceived in the early years of research. Some of these early uses for lasers are beginning to come to fruition now.

The second innovation was the invention of tunable solid state lasers, such as Cr:BeAl₂O₄ [2] and Ti:Al₂O₃ lasers [3]. Although tunable lasers such as Ni:MgF₂ and Co:MgF₂ [4] were discovered earlier, their low gain and cryogenic cooling discouraged wide acceptance. Conversely, Cr:BeAl₂O₄ operated in

the near visible region at room temperature and was reasonably efficient for a flash lamp pumped laser. Ti:Al₂O₃, although usually laser pumped, was quite efficient and possessed a very wide tuning range.

The third innovation was the invention of the diode pumped laser, primarily the diode pumped Nd:YAG laser. Diode pumping was recognized early on, as offering both higher efficiency and reliability. Light emitting diodes with aggressive cooling were employed initially [5]. With redesign, operation at room temperature was achieved [6]. However, laser diodes, instead of light emitting diodes, made diode pumped lasers practical. Laser diodes have 2 orders of magnitude lower divergence as well as an order of magnitude smaller bandwidth than light emitting diodes, greatly enhancing laser efficiency. Compact disk players also needed laser diodes with a similar wavelength. Commercial demand for these devices advanced individual laser diode technology. Forming these individual laser diodes into useful laser diode arrays was expedited by a government sponsored build of 2 lasers with nominal Joule per pulse output.

The fourth innovation was the fiber laser. This concept was also demonstrated in the early stages of laser research [7]. A major impetus for optical fiber development came from the optical communications sector which required low loss optical fiber. Er doped fiber laser amplifiers [8] coupled with low loss fibers fueled growth of this technology. Fiber lasers offer

the advantages of high efficiency and good beam quality at high average power.

Solid state lasers are discussed here from an efficiency point of view. Efficiency factors are used to characterize the laser processes. Often efficiency factors depend on energy transfer processes, some in rather subtle ways such as concentration quenching. When possible, closed form approximations for these efficiency factors are given. In turn, efficiency factors are used to calculate a threshold and slope efficiency. Often there is sufficient uncertainty in values of the laser parameters that more accurate predictions than these first order predictions are not warranted.

Energy storage and pulse repetition frequency:

Energy storage allows optical pump energy to be delivered over long time intervals and released in a single high peak power or Q-switched pulse. High peak power pulses are desired for many applications ranging from laser material processing to nonlinear optics. Solid state laser power can be delivered in any pulse format from continuous laser operation to GHz pulse repetition frequencies and beyond.

Different pulse repetition frequencies are achieved using different modes of laser operation. For low pulse repetition frequencies, on the order of 100 Hertz or less, electrical energy is stored in the power supply and delivered to an optical pump source over a time interval on the order of 1.0 ms. The laser output pulse may begin as soon as the pump delivers sufficient energy to achieve threshold and can last for the remaining duration of the pump pulse. Transition to a quasi steady state output occurs through a series of oscillations referred to as relaxation oscillations. Pulsed quasi steady state operation is referred to as normal mode operation. Conversely, laser operation may be inhibited through the activation of a Q-switch. A Q-switch inhibits lasing until the end of the pump pulse. At the end of the pump pulse, the energy stored in the laser material is released in a single, high peak power pulse. This mode of laser operation is referred to as Q-switched operation. A pulsed pump is used for pulse repetition frequencies up to ≈ 1.0 kHz.

For higher pulse repetition frequencies, the pumping is continuous and the energy is stored in the active atom. The Q-switch prevents laser action until the appropriate instant. When, the Q-switch opens, a short pulse is generated. The Q-switch closes and the process is repeated. This mode of operation is usually appropriate between roughly 1.0 kHz and 100 kHz.

For even higher pulse repetition frequencies, cavity dumping can be employed. Here pumping is continuous but the energy is stored in the optical field of the resonator rather than in the laser material. At the appropriate time, an optical modulator is activated, dumping the energy out of the resonator in as little as a round trip time interval. The optical modulator is then deactivated and the optical field energy recovers. Cavity dumping is appropriate for pulse repetition frequencies between about 100 kHz and a few MHz.

For yet higher pulse repetition frequencies, mode locking can be employed. By locking resonator modes together, a pulse is generated which circulates around the resonator. Every time it encounters the output coupler, a fraction of its energy is coupled out. The remaining pulse then propagates through the gain medium and the optical field energy recovers. Mode locking is appropriate for pulse repetition frequencies above about 10 MHz. The upper limit is limited only by how short the resonator can be made.

Transition metal and lanthanide series lasers:

Solid state lasers fall into 2 general categories depending on the active atom. Transition metal lasers have active atoms from the fourth row of the periodic table spanning the elements from Ti to Ni and include Cr. Lanthanide series lasers have active atoms from the sixth row of the periodic table of the elements and span the elements from Ce to Yb and include Nd.

Transition metal lasers use transitions between 3d electron levels. The 4s and 4p electrons are used in the bonding process. Thus, 3d electrons are exposed to the electric field of the crystal. The crystal field has a large effect on the energy levels and the transition rates. Laser transitions are usually vibronic in nature. This implies the emission of a photon is coupled with

the simultaneous emission of a phonon. Because the phonon spectrum can be wide, transition metal lasers often have wide tuning ranges and absorption features.

Lanthanide series lasers employ transitions between the 4f electron levels. The 5s and 5p electron shells are completely filled. A 4f and the 6s electrons participate in the bonding process. Thus, because of the shielding effect of the filled 5s and 5p electrons, the electric field of the crystal produces only a small perturbation on the energy levels. Because of this, the transitions are usually relatively narrow, in absorption and emission. Electron orbitals appear in Figure 3.

The product of the emission cross section, σ_e , line width, $\Delta\nu$, and upper laser manifold lifetime, τ_2 , is limited. This relationship is known as the Fuchtbauer-Ladenberg relation,

$$\sigma_e \Delta\nu \tau_2 = (\lambda_L^2 / 4\pi^2) (g_2 / g_1)$$

where g_i are the degeneracies of the upper and lower levels. Because of their wide line widths, transition metal lasers usually possess a small emission cross section, for example Cr:BeAl₂O₄, or short upper laser manifold lifetime, for example Ti:Al₂O₃. Conversely, lanthanide series lasers tend to have larger emission cross sections and longer upper laser lifetimes but a limited line width.

Manifolds and energy levels:

Manifolds are groups of closely spaced energy levels. Close spacing of the energy levels provides a rapid thermalization time constant, on the order of a picosecond. The fractional population of each level in the manifold is described by a Boltzmann or thermal occupation factor. Laser transitions occur between a pair of individual levels in the participating manifolds. When the laser pulse length is long compared with the thermalization time constant, the entire manifold can contribute to the laser output pulse. Therefore, laser dynamics are usually employed to describe manifold rather than the energy level population densities. Due to their inhomogeneous nature, glass laser materials have ill defined energy levels.

Gain is usually written in terms of manifold population densities. In terms of the upper and lower laser level population densities, N_{2L} and N_{1L} , the small signal gain, G_0 , is

$$G_0 = \exp[\sigma(N_{2L} - N_{1L})l] = \exp[\sigma(Z_2 N_2 - Z_1 N_1)l]$$

where Z_i and N_i are the appropriate Boltzmann factor and manifold population density, respectively. The effective emission cross section, σ_e , often absorbs the Boltzmann factor and the small signal gain becomes $\exp[\sigma_e(N_2 - Z_1 N_1 / Z_2)l]$.

True 4 level lasers are more efficient than true 3 level lasers. With a 3 level laser, the transition of an active atom from the upper laser level into the lower laser level decreases the population inversion by 2. That is, there is 1 less active atom in the upper laser level and 1 more active atom in the lower laser level. With a 4 level laser, the transition of an active atom from the upper laser level into the lower laser level decreases the population inversion decreases by 1. That is there is 1 less active atom in the upper laser level. An active atom in the lower laser level quickly disappears.

Quasi 4 level lasers have a nontrivial thermal population in the lower laser level. Often, the vast majority of active atoms are either in the upper laser manifold or the ground state manifold. This is the case for the following transitions: Nd ⁴F_{3/2} to ⁴I_{9/2} at 0.95 μ m, Er ⁴I_{13/2} to ⁴I_{15/2} at 1.66 μ m, Ho ⁵I₇ to ⁵I₈ at 2.09 μ m, Tm ³F₄ to ³H₆ at 2.01 μ m, and Yb ³F_{5/2} to ³F_{7/2} at 1.03 μ m. In these cases, N_1 can be replaced by $(C_N N_S - N_2)$ where C_N is the concentration of active atoms and N_S is the density of available sites. The gain becomes

$$G_0 = \exp[\sigma_e(\gamma N_2 - (\gamma-1)C_N N_S)l]$$

where γ is defined as $(1 + Z_1/Z_2)$. Thus, the transition of an active atom decreases the population inversion by γ . For all of the above transitions, this quantity is much closer to 1 than 2. As a result, these transitions are referred to as quasi 4 level lasers. For a quasi 4 level laser, optical transparency is achieved when the upper manifold population density reaches N_{2T}

$$N_{2T} = C_N N_S (\gamma - 1) / \gamma$$

Below this population density, loss is greater than gain, and above gain is greater than loss. For 4 level lasers, the relations apply if N_{2T} is set to 0.

Product Of Efficiencies Approach:

Laser efficiency can be well approximated by a linear relation characterized by a threshold and slope efficiency. The slope efficiency can be directly approximated by a product of the efficiencies of the various processes, the pump efficiency, the efficiency coupling the pump radiation to the laser material, the absorption efficiency, and so forth. Threshold can be approximated by using the product of efficiencies to determine the population inversion. Knowing the population inversion and the losses allows prediction of the threshold. Each of these efficiency factors are described below.

Pump Source Efficiency:

Solid state lasers are pumped with an optical source. In the early days, this source was an electrical discharge, usually in an inert gas Xe, Kr, or rarely Ar. Flash lamps provide pulsed excitation and arc lamps provide continuous excitation. Arc lamp conversion of electrical to optical power, η_p , can be efficient, [9] 0.54 for Xe and 0.45 for Kr. Lamp efficiency depends on the lamp geometry and fill pressure. Efficiency of flash lamps depends on the discharge circuit as well. Flash lamps can be driven by discharging a capacitor, C, through an inductor, L. Depending on the circuit, the discharge can be under damped, critically damped, or over damped. Efficiency is usually highest with a critically damped circuit. At high currents, the flash lamp voltage is proportional to the square root of the current. In this situation, critical damping is achieved when the damping parameter, α , is 0.8. The damping parameter is [10]

$$\alpha = (K_0/V^{1/2})(C/L)^{1/4}$$

where K_0 , the flash lamp impedance parameter, is $1.13(1/A^{1/2})$. Here l is the arc length and A is the lamp cross section area. If critically damped, the discharge appears much like a half sinusoid with a pulse length of $3(LC)^{1/2}$. Flash lamps can also be driven with a

nearly square pulse discharge circuits by monitoring the flash lamp current and maintaining it.

The advantages of flash and arc lamps are low cost, high pulsed energy, and a good conversion of electrical to optical power. The disadvantages are a wide spectral bandwidth, low brightness, and limited lifetime. High energy pulsed flash lamps behave like black body radiators although there is some broad line features in the near infrared. The back body emission spectrum of a flash lamp is a particularly poor match for the narrow absorption features of lanthanide series lasers. Transition metal lasers absorb a considerably greater fraction of the black body radiation but are still not highly efficient. At lower energies, broad line features in the near infrared become more prominent. Arc lamp spectra have weak black body features and strong line features. Some overlap occurs between Kr arc lamp emission and Nd:YAG absorption spectra.

Laser diodes can convert electrical power to optical power with efficiency, η_p , as high as 0.7. Laser diodes can have a narrow spectral bandwidth and high brightness. Laser diodes can be tuned by varying the composition. Initially, laser diodes were fabricated using $Ga_xAl_{(1-x)}As$. Wavelength tuning was achieved by varying the ratio of Ga to Al. Later, quantum well laser diodes were tuned by varying the width of the quantum well. Laser diode arrays for pumping solid state lasers are available between about 0.67 to 0.69 μm using GaAlInP, 0.78 to 0.84 μm using InGaAsP, as well as 0.90 to $>1.00 \mu m$ using InGaAs. Spectral bandwidths can be as small as a few nm, commensurate with the absorption features of many lanthanide series lasers. Narrow spectral band width diodes, tuned to strong absorption features, provide much higher absorption efficiencies.

The small emission area of a laser diode provides for high brightness output. Emission areas of single stripe laser diodes are on the order of 1.0 by 200 μm . In the 1.0 μm plane, the beam quality can approach the diffraction limit but the beam is highly divergent. The beam is often nearly collimated in this plane by using a fiber lens. High brightness enhances high coupling efficiency. In turn, this enables fiber lasers and end pumped lasers. For higher power, laser

diodes are often fabricated in bars with 19 or 20 laser stripes located on a 10 mm bar. For even higher pump powers, bars can be stacked into arrays. However, optical methods of coupling the laser diode bars or arrays into the laser material must be found.

Advantages of laser diodes include a narrow spectral bandwidth that is tunable to strong absorption features, high brightness, and a long lifetime, often in excess of several 1000 hours. Disadvantages include a relatively high cost. However, as demand for diode pumped lasers increases, the cost of laser diode arrays continues to decrease.

Coupling Efficiency:

Coupling efficiency describes the fraction of the photons emitted by the source that enter into the laser material. It is usually approximated as being independent of the pump wavelength which is an excellent approximation for laser diodes. Coupling methods are dependent on the type of pump source. Fresnel reflections must be taken into account in addition to the efficiency factors described below.

An early innovation coupled linear lamps to laser rods employing elliptical, specularly reflecting, cavities. A linear flash lamp is placed at or near a focus of the ellipse and the laser rod is placed near the other focus. A property of an ellipse is a ray emitted at a focus will travel to the other focus after a single reflection from the elliptical surface, see Figure 2. Because of the finite size of the lamp, not all of the rays will impinge on the laser material. Given an ellipse with semi major axis, a , and semi minor axis, b , the coupling efficiency η_C , can be approximated as

$$\eta_C = [\alpha_0 + (c/d)(\theta_0 - \theta_1)]/\pi \quad \text{where}$$

$$\cos(\alpha_0) = [1 - ((1 - e^2)/2)(1 + c/d)]/e$$

$$\sin(\theta_0) = d \sin(\alpha_0)/c$$

$$\sin(\theta_1) = d/(4ae)$$

where c and d are the diameter of the laser rod and the lamp, respectively and e is the ellipticity [11]. When the ellipticity is small and the ellipse is large, pumping

tends to be nearly uniform over the lateral surface of the laser rod. When the ellipse is small, the coupling efficiency can be more efficient because radiation not absorbed in the first single pass through the laser rod can make a second pass. However, the pumping tends to stray further from uniform as the ellipse becomes smaller and more eccentric. Specular cavities are plated with Ag or Au. The reflectivity of the plating must be included in the coupling efficiency. Au is highly reflective to $\approx 0.6 \mu\text{m}$ and does not tarnish. Ag is highly reflective to $\approx 0.4 \mu\text{m}$.

Lamps can also be coupled to laser rods by using diffuse, but highly reflecting cavities. Some materials, such as BaSO₄ or ceramics, have a diffuse reflectivity >0.99 . Because of the high reflectivity of the cavity, coupling efficiency can be approximated

$$\eta_C = S_L \beta_L / \sum S_i \beta_i$$

where S_L and β_L are the area and capture coefficient of the laser rod, respectively. The summation is over all areas of the cavity. Areas in the cavity that represent a loss, besides the laser rod, include holes that allow coolant and the flash lamp to enter the cavity [12]. Coupling efficiencies have been shown to approach 0.75. Advantages of the diffusely reflecting cavity are their wide spectral reflectivity and tarnish free nature.

Laser diodes can easily and efficiently coupled to a laser rod by arranging the laser diode bars around the periphery of the laser rod and parallel to the axis. The coupling efficiency can approach 1.0 in this case. This approach works well if only a modest amount of pump energy is required. By way of comparison, a flash lamp can easily deliver 50 J of optical energy to a 5.0 by 50 mm laser rod in a 200 μs pulse while laser diodes can deliver about 1.5 J. Higher pump fluences are possible using the high brightness of laser diodes.

Lens ducts can efficiently increase the pump fluence. A lens duct is a combination of a lens and a tapered waveguide. The lens portion of the lens duct essentially focuses the pump radiation on the small end of the lens duct. However, to obtain the highest efficiency, the length of the lens duct should be [13]

$$l = 0.92r_d n_d / (n_d - 1).$$

In a typical application, the pump energy from a laser diode array is concentrated to end pump a laser rod or laser disk. Pump rays that are not too divergent will be totally internally reflected by the tapered sides of the device. Although the reflection saves the ray, the divergence increases. After several reflections, the incident angle may no longer exceed the total internal reflection or the ray may be reflected back toward the pump. Efficiency of a lens duct depends on the ratio of the input to output sizes and the divergence of the source. If the source is a laser diode array, a fiber lens is often employed to decrease the divergence of the fast axis. For a lens duct with an input size of 15 by 125 mm coupling into a 6.35 mm rod, the calculated efficiency was 0.78 calculated with no antireflection coating and 0.92 antireflection coatings [13].

Fiber optics can also symmetrize the output of laser diode bars to enhance coupling efficiency. An optical fiber is coupled to each of 19 diode stripes on a laser diode bar. The fibers are gathered into a close pack hexagonal fiber bundle. Diameter of this fiber bundle can be as small as 600 μm with a numerical aperture of 0.14. Output from this fiber bundle can be coupled directly or coupled with a lens to end pump a laser rod or disk.

A pair of tilted and offset mirrors can be used to rearrange the output of a laser diode bar to a more convenient format for concentrating pump radiation on the laser material [14]. Before the pump radiation encounters the mirrors, it must be collimated. A fiber lens collimates the pump radiation along the fast axis. The fiber lens is often the optic with the highest loss. After lensing, the pump radiation has high divergence and large emitting dimension in the same plane. By employing a pair of tilted and offset mirrors, a line of diode stripes is imaged to a stack of stripes. This puts the high divergence in the plane with a small emitting dimension. This enhances the coupling efficiency significantly. If the mirrors are 0.998 reflective, the stacking efficiency of the mirrors can be as high as 0.96. In practice, stacking efficiency exceeds 0.92. Overall efficiency of this device is roughly 0.75.

For fibers, coupling efficiency is often referred to as launch efficiency. Coupling is aided by using an undoped inner cladding that is large compared with the core and has a large numerical aperture. The laser diode can be focused into the inner cladding where it is contained by total internal reflection. As the pump radiation propagates, it encounters a doped core where it is absorbed. Coupling efficiency is that fraction of the diode radiation within the radius and numerical aperture of the inner cladding.

Absorption Efficiency:

Absorption efficiency describes conversion of incident pump photons to atoms in the upper laser level. The pump source is characterized by a relative spectral distribution, $P(\lambda)$, and the laser material is characterized by an absorption coefficient, $\beta_a(\lambda)$. The pump photons have a distribution of incident angles, $F(\theta, \phi)$, and travel a path length, $l(\theta, \phi)$, in the laser material which depends on the incident angles, θ and ϕ . Given this, the absorption efficiency is [15]

$$\eta_A = \frac{\int_{\lambda_1}^{\lambda_2} \int_0^{\pi/2} \int_0^{\pi/2} (\lambda/\lambda_L) \text{PF}(1 - \exp(-\beta_a l)) \sin(\theta) d\theta d\phi d\lambda}{\int_{\lambda_1}^{\lambda_2} \int_0^{\pi/2} \int_0^{\pi/2} \text{PF} \sin(\theta) d\theta d\phi d\lambda}$$

where λ is the pump wavelength and λ_L is the laser wavelength. Every pump photon absorbed by a given pump manifold has the same probability of producing an atom in the upper laser level. However, the pump photons with longer wavelengths are more efficient because they have less energy. The factor $1/\lambda_L$ is used to normalize so the efficiency is dimensionless

To calculate absorption efficiency, absorption coefficients for the laser material are measured as a function of wavelength, typically with a resolution of 0.1 nm for lanthanide series lasers. For birefringent materials, absorption spectra are taken as a function of polarization as well. A typical laser diode emission spectrum can be numerically manipulated to vary the emission spectrum in a systematic way to determine the optimum pump wavelength. Once having found

the optimum wavelength, absorption efficiency can be calculated as a function of a characteristic length, such as rod radius. This has been done for diode and flash lamp pumped Nd laser materials [15,16]. For narrow spectral bandwidth laser diodes or favorable coupling schemes the absorption efficiency can be >0.9. This formalism is directly applicable for diode pumped lasers and lasers where all pump manifolds decay to the upper laser manifold, such as Nd.

To achieve good absorption efficiency for fiber lasers, mode mixing is needed within the inner cladding. Without mode mixing, pump radiation can spiral around the inner cladding and never encounter the doped core. Mode mixing can be achieved by introducing some feature to break the symmetry such as: a core offset from the center, flats ground on the lateral surface of the inner cladding, inner cladding geometries other than circular, and so forth.

Quantum Efficiency:

Quantum efficiency relates the probability of an absorbed photon producing an atom in the upper laser level. Photons absorbed in a pump manifold may bypass the upper laser manifold by radiative decay to a manifold that is lower. In all probability, the decay from the pump to the upper laser manifold occurs by nonradiative transitions. If the upper laser manifold is directly below the pump manifold, the quantum efficiency is approximately

$$\eta_Q = (1/\tau_{NR}) / ((1/\tau_{NR}) + (1/\tau_{RAD}))$$

τ_{NR} and τ_{RAD} are the pump manifold nonradiative and radiative lifetime. If there are intervening manifolds, quantum efficiencies are calculated for each manifold. The quantum efficiency of the laser is the product of the manifold to manifold quantum efficiencies.

Quantum efficiency also describes the results of an energy transfer process. Energy transfer is an exchange of energy between manifolds of 2 atoms that are physically close. 1 of the atoms transitions to a lower manifold and the neighboring atom transitions to a higher manifold. To maintain conservation of energy, the transitions should be nearly resonant. When energy transfer is a dipole-dipole interaction,

energy transfer rates depend on the distance between the interacting atoms to the inverse sixth power.

Energy transfer contributions to the quantum efficiency are illustrated by the Ho:Tm system. Rate equations describing the energy transfer processes where manifold 2 is pumped are

$$dN_2/dt = -N_2/\tau_2 - P_{28}N_2N_8 + P_{71}N_7N_1 + R_2$$

$$dN_7/dt = -N_7/\tau_7 - P_{71}N_7N_1 + P_{28}N_2N_8$$

$$N_1 + N_2 = C_T N_S$$

$$N_7 + N_8 = C_H N_S .$$

where 1, 2, 7, and 8 denote the Tm ³H₆, Tm ³F₄, Ho ⁵I₇, and Ho ⁵I₈ manifolds. P₂₈ and P₇₁ are the energy transfer parameters. The rate that energy transfers out of manifold 2 is directly dependent on the population density in the donating manifold, manifold 2, as well as the population density in the accepting manifold, manifold 8. Decay, τ_2 , is in competition with energy transfer. Concentrations can be selected to optimize the population density in the upper laser manifold, N₇. Quantum efficiency in this case is N₇/R₂ τ_1 .

Energy transfer parameters can be calculated for crystalline laser materials. Early energy transfer parameter calculations were applicable to random materials [17,18]. Because of the random nature of the material, an average over the orientation of the dipoles and separation of the dipoles was performed. Because of the R⁻⁶ dependence of the energy transfer rate on the dipole separation, the choice of the closest separation is highly critical. Measured absorption and emission spectra were utilized to calculate the energy transfer parameters. In more recent calculations, the energy transfer parameters were calculated utilizing the dipole orientation and separation dictated by the crystal lattice [19]. These calculated energy transfer parameters were employed to predict the performance of a Ho:Tm:YLF amplifier. These predicted results were supported by extensive experimental data [20]. The ability to calculate the energy transfer parameters is important because the measurement of these parameters can be difficult.

Using energy transfer to increase absorption efficiency was an early innovation [21]. Some solid state lasers do not have commercially available laser diodes for pumps. Lasers employing energy transfer pumping are: Yb $^3F_{5/2}$ to Er $^4I_{11/2}$, Tm 3H_4 to 3F_4 , Tm 3F_4 to Ho 5I_7 , Er $^4I_{13/2}$ to Tm 3F_4 , and Cr to Nd.

Storage Efficiency:

Storage efficiency describes the fraction of the stored energy that remains available at the time the laser pulse is emitted. If energy is stored in the upper laser manifold for Q-switched operation, the storage efficiency, η_s , is

$$\eta_s = (\tau_2/\tau_1)[1 - \exp(-\tau_1/\tau_2)] \text{ or } (\tau_Q/\tau_2) [1 - \exp(-\tau_Q/\tau_2)]$$

Here τ_2 is the upper laser level lifetime, τ_1 is the pump pulse length, and τ_Q is the time interval between the Q-switched pulses. The former is applicable to pulsed pumping while the latter is applicable to continuous pumping. If the energy is stored in the optical field, the relevant time constant is the photon lifetime in the resonator, $-\ln(R_M R_L)/\tau_{RT}$. Here τ_{RT} is the round trip time interval, R_M is the output mirror reflectivity and R_L represents the optical losses. If the laser operates continuously, the storage efficiency is not relevant. If the storage time interval is less than 2/3 of the relevant time constant, the storage efficiency greater than 0.73. This result is valid for low population densities.

The upper laser level lifetime depends on the concentration when self quenching is operative. Self quenching is an energy transfer process by which an atom in the upper laser manifold transitions to a lower manifold and a similar atom in the ground manifold transitions to a higher manifold. As an example, a Nd, atom in the $^4F_{3/2}$ manifold transitions to the $^4I_{15/2}$ manifold and a nearby Nd atom in the $^4I_{15/2}$ manifold transitions to the $^4I_{9/2}$ manifold. Dynamics of the $^4F_{3/2}$ manifold population density, N_4 , are

$$dN_4/dt = -N_4/\tau_4 - P_{41}N_4N_1 \approx -(1/\tau_4 + P_{41}C_N N_S) N_4$$

where P_{41} is the energy transfer parameter and τ_4 is the lifetime. Analysis is complex because averaging over possible local environments of the Nd atom is needed.

Only Nd atoms that have a Nd atom in the nearest similar neighbor position have a significant rate of self quenching. This is a result of the energy transfer process depending on the distance between the participating atoms to the inverse sixth power. However, the quantum of energy can diffuse from Nd atom to Nd atom much faster, ≈ 1000 times faster. Diffusion is much faster because of the guaranteed energy overlap between the donating and accepting atoms, both Nd in this case. With rapid diffusion, the quantum of energy can wander in the crystal until it finds a doublet, a pair of Nd atoms in nearest similar neighbor positions. Encountering a doublet does not guarantee self quenching will occur. The quantum of energy may be required to visit doublets many times before self quenching occurs. If the time interval required for several visits is long compared with the fluorescent lifetime, self quenching will not be a major factor. Here, lifetime is nearly independent of the concentration. As the concentration increases, diffusion becomes fast and doublets become more common. Here, the inverse lifetime is nearly linearly related to the concentration, see Nd:YAG in Figure 3. Conversely, Nd:YLF, with a long lifetime, shows a linear dependence even at low concentrations.

As the population density increases, the rate of loss from the upper laser level increases. During the pumping process, at rate R_2 , the population density is

$$dN_2/dt = R_2 - N_2/\tau - \beta N_2^2$$

where τ is the effective lifetime. The nonlinear term, β , could be caused by amplified spontaneous emission or by up conversion. In the former case, replace β by $\sigma_{ea}l_a/\tau$ where σ_{ea} is the emission cross section averaged over all possible transitions originating from the upper laser manifold and l_a is the average length traveled by spontaneously emitted photons. This approximation is highly useful because the first term depends only on the laser material and the second term depends only on the geometry of the pumped laser volume [22]. In the latter case, replace β by $(2-\eta_Q) P_{22}$ where η_Q is the quantum efficiency of the excited manifold and P_{22} is the energy transfer parameter. The factor of 2 arises because 2 Nd atoms in the upper laser manifold are

lost in the process. In either case, the storage efficiency can be shown to be [22]

$$\eta_S = (2\tau/\tau_i)(1 - \exp(-r\tau_i/\tau))$$

$$/[(r + 1) + (r - 1) \exp(-r\tau_i/\tau)]$$

$$r = [1 + 4R_2\tau\sigma_{ea}l_a]^{1/2} \text{ or } [1 + 4(2-\eta_Q)P_{22}R_2\tau^2].$$

Up conversion and amplified spontaneous emission produce the same behavior through first order.

Extraction Efficiency:

The dynamics of the lasing process must be solved to determine the extraction efficiency. Laser dynamics can be described using rate equations to describe the population density of the upper and lower laser manifolds, N_2 and N_1 , and the photon field, N_P . For quasi 4 level lasers, the rate equations are [23]

$$\frac{\partial N_2}{\partial t} = -\frac{N_2}{\tau_2} + R_2 - \sigma(Z_2N_2 - Z_1N_1) \frac{c}{n} N_P$$

$$\frac{\partial N_1}{\partial t} = +\frac{N_2}{\tau_2} - R_2 + \sigma(Z_2N_2 - Z_1N_1) \frac{c}{n} N_P$$

$$\frac{\partial N_P}{\partial t} + \frac{c}{n} \frac{\partial N_P}{\partial z} = \sigma(Z_2N_2 - Z_1N_1) \frac{c}{n} N_P$$

where τ_2 is the lifetime, R_2 is the pumping rate, c is speed of light, and n is the refractive index. In many cases, the active atoms are either in the upper laser manifold or the ground manifold, that is

$$N_1 + N_2 = C_N N_S.$$

In this case, the second equation becomes redundant. When the output mirror reflectivity is larger than ≈ 0.5 , the variation of the photon density along the length of the resonator is relatively small. Integrating over the length of the resonator and adding a loss term yields

$$\frac{\partial N_2}{\partial t} = -\frac{N_2}{\tau_2} + R_2 - \frac{2\sigma_e l_c}{n} \frac{c}{2l_c} [\gamma N_2 - (\gamma - 1)C_N N_S] N_P$$

$$\frac{\partial N_P}{\partial t} = 2\sigma_e l_c \frac{c}{2l_c} [\gamma N_2 - (\gamma - 1)C_N N_S] N_P + \frac{c}{2l_c} \ln(R_M R_L) N_P$$

The coupled equations can be solved to yield the population density N_2 . Multiplying by the photon energy and the pumped volume yields the extraction efficiency $(E_{20} - E_{2T})/(E_{20} - E_{2T})$

$$\frac{E_{20} - E_{2F}}{E_{20} - E_{2T}} = \frac{-(E_{STH} - E_{2T})}{(E_{20} - E_{2T})} \ln \left[1 - \frac{E_{20} - E_{2F}}{E_{20} - E_{2T}} \right]$$

where E_{2F} is the stored energy at the end of the pulse

$$E_{20} = \eta_P \eta_C \eta_A \eta_Q \eta_S E_P = \pi a_r^2 l h c N_{20} / \lambda_L$$

$$E_{2T} = \pi a_r^2 l h c N_{2T} / \lambda_L$$

$$E_{STH} = -\ln(R_M R_L) / (2\sigma_e \gamma l) + E_{ST}$$

E_{STH} is the stored energy at threshold. Calculation of the extraction efficiency introduces a threshold. For the solution to be real, $(E_{20} - E_{2T})/(E_{STH} - E_{2T})$ must be greater than 1.0. Figure 4 is the relation between extracted energy, $(E_{20} - E_{2F})$, and stored energy above optical transparency. $(E_{20} - E_{2T})/(E_{STH} - E_{2T})$ is in essence the number of times over threshold. For 4 level lasers, the same relation hold with E_{2T} set to 0.

Laser output energy, E_{LO} , can be expressed as

$$E_{LO} = \frac{w^2}{a_r^2} \frac{\ln(R_M)}{\ln(R_M R_L)} (E_{20} - E_{2F})$$

where $(w/a_r)^2$ represents the overlap efficiency and $\ln(R_M)/\ln(R_M R_L)$ is the fraction of extracted photons that appear in the laser output. The laser beam is assumed uniform over a cylinder with radius w and the upper manifold population density is assumed uniform over a cylinder with radius a_r . The relation between laser output energy for Q-switched operation and the pump energy, and therefore the input energy, is not strictly linear but somewhat less than linear. Deviation from linearity is relatively minor over a limited range. As the pumping is increased, extraction efficiency increases and the slope between extracted energy and stored energy approaches 1.0.

Conversely, the relation between laser output energy for normal mode operation and pump energy is somewhat greater than linear. Near threshold, lasing begins near the end of the pump pulse. Thus storage efficiency is included in a calculation of the threshold. Above threshold, lasing begins earlier in the pump pulse. Thus, storage efficiency increases as pumping increases and approaches 1.0. Under normal mode operation, 2 operating regimes exist, the approach to threshold, where no lasing occurs, and quasi steady state lasing. The transition between the 2 operating regimes where relaxation oscillations occur appears in Figure 5. In multimode lasers, many sets of relaxation oscillations can occur making the laser output appear to be random spikes.

The threshold and slope efficiency under continuous operation are found when the temporal derivatives vanish. Solving the remaining equations for the population densities yields the laser output power, P_{LO} , [23]

$$P_{LO} = \pi w^2 l \frac{hc}{\lambda_L} \frac{\ln(R_M)}{\ln(R_M R_L)} (R_2 - R_{2TH})$$

$$R_2 = \eta_p \eta_c \eta_A \eta_Q P_p \lambda_L / (hc \pi a_r^2 l)$$

$$R_{2TH} = [(\gamma - 1) C_N N_S - \ln(R_M R_L) / (2\sigma_e l)] / (\gamma \tau_2).$$

Pumping is assumed uniform over a cylinder with a radius a_r and length l . Substituting R_2 and R_{2TH} into the expression for P_{LO} yields the threshold and slope efficiency.

Overlap Efficiency:

Choice of laser geometry can have a profound effect on the efficiency and average power capability. Historically, laser geometries were often in the form of cylinders, as shown in Figure 6. Cylindrical laser rods are compatible with linear flash lamps. They can also be useful for end pumping of laser materials with low absorption coefficients. Laser rods pose a hard aperture making extraction of the population inversion near the periphery of the laser rod more difficult. If laser operation is restricted to TEM₀₀ modes, the beam radius is often set at about 0.6 of the laser rod radius.

This restricts the overlap efficiency to roughly 0.36. In addition, cooling was usually achieved by flowing coolant over the lateral surface of the laser rod. This leads to radial thermal gradients and thermal lensing that degrades beam quality and limits average power. This geometry is capable of generating high energy pulses and is relatively easy to fabricate.

Slab lasers are an innovation that promotes higher beam quality and average power [24]. The cross section of the laser slab is rectangular. The pump is introduced through a single side or a pair of opposing sides. The laser beam is reflected by total internal reflection from these sides. Because of the rectangular geometry, thermal focusing is minimized. The laser slab presents hard apertures to the laser beam. If TEM₀₀ operation is desired and the beam radius is restricted to 0.3 of the square cross section dimension the overlap efficiency can approach 0.5. The overlap efficiency can be good because the slab geometry can extract energy from the periphery at least in 1 dimension. This geometry is capable of generating high energy pulses. However, fabrication is complicated because of the geometry and the need for high optical quality laser material and lateral surfaces. Total internal reflection and tapered ends make this geometry susceptible to parasitic lasing if corrective measures are not employed.

Disk lasers can present a very high overlap efficiency. Disk lasers are naturally compatible with an end pumping geometry. The pump beam radius can be much smaller than the radius of the disk. Thus the laser beam can completely overlap the pump beam leading to high overlap efficiency. However, use of a large laser beam radius reduces the gain. Therefore, optimum efficiency is a compromise between overlap efficiency and extraction efficiency. For small disks, the limited volume may restrict the available energy per pulse. Either radial or longitudinal heat extraction can be used but the longitudinal method is preferred to minimize thermal lensing.

Optical fibers can present a very high overlap efficiency. In a typical application, the fiber laser consists of a small core, $\approx 10 \mu\text{m}$, and inner cladding,

≈100 μm, and an outer cladding. Pump radiation is introduced in the inner cladding and confined there. The active atoms are confined to the core where the pumping is nominally uniform. The laser beam is a guided wave that completely fills the core and leaks into the inner cladding. This produces a very high overlap efficiency. Because of the small core and the possibility of long lengths, both high gain and high overlap efficiency are possible. Guided waves in a small core fiber produce good beam quality. A high surface to volume ratio and the guided wave nature allow good beam quality even at high average power. Fiber lasers have small core sizes and limited active volumes which limit the energy per pulse.

Examples:

Using the above models, laser performance can be calculated given the requisite spectroscopic parameters. Among the requisite spectroscopic parameters are: laser wavelength, upper laser level lifetime, upper and lower laser manifold Boltzmann factors, emission cross section, and line width. The refractive index is described with a 2 pole Sellmeier equation, that is an ultraviolet and an infrared pole.

$$n^2 = A + B\lambda^2/(\lambda^2 - C) + D\lambda^2/(\lambda^2 - E)$$

Spectroscopic parameters for several common laser transitions are listed in Table 1. Sellmeier constants for 5 common laser materials are listed in Table 2.

Thermal and mechanical properties of a laser material dictates average power considerations such as thermal lensing and average power limits. Space does not permit describing these effects. Suffice it to say there are both a thermal expansion and a thermo-optic contributions to thermal lensing. Laser materials with low values for these coefficients are preferred. Better yet, select a laser material so that these contributions tend to cancel. YLF is such a laser material.

Thermal shock, R_T is useful for describing the resistance to thermal fracture. It is defined as

$$R_T = (1 - \nu)k_C S_T / \alpha E.$$

ν is Poisson's ratio, k_C is the thermal conductivity, S_T is the tensile yield strength, α is the coefficient of thermal expansion, and E is Young's modulus. The tensile yield strength tends to be higher for oxides than fluorides but is highly dependent on the surface finish. Thermal and mechanical properties of 5 laser materials appear in Table 3.

Performance of different laser materials and designs will be compared by noting their thresholds and slope efficiencies. Flash lamp pumped lasers quote electrical to optical data. Diode pumped lasers usually quote optical to optical data. Common laser transitions are shown in Figure 7. Wavelength of some lasers, like Ho, depend on the concentration of the active atom. The wavelength can be predicted with a knowledge of the losses and the concentration and length product [19].

A comparison of 4 Nd laser materials under the same flash lamp pumping was performed for the 1.06 and 1.32 μm transitions [25]. Nd:YAG had a threshold of 5.3 J and slope efficiency of 0.020 when at 1.064 μm as well as a threshold of 5.0 J and slope efficiency of 0.012 when at 1.338 μm. Nd:YLF had a threshold of 7.0 J and slope efficiency 0.012 when at 1.047 μm as well as a threshold of 7.5 J and a slope efficiency of 0.007 when at 1.313 μm. Utilizing a completely different design, Nd:YAG achieved a threshold of 12 J and slope efficiency of 0.010 for TEM₀₀ operation at 0.946 μm [26]. When a need arose for a laser operating at 0.9441 μm, an innovative method referred to as compositional tuning [27] was developed. Using nonstoichiometric isomorphs of YAG, tuning from, 0.938 to 0.946 μm was achieved.

A diode pumped, continuous, Nd:YAG laser achieved a 6 W output with a threshold of 3.0 W and slope efficiency of 0.55 [14]. A side pumped design, where lens ducts concentrated laser diode radiation on the lateral surfaces of the laser rod, achieved a 320 W output with a threshold of 200 W and a slope efficiency of 0.36, electrical to optical [28].

Nd:YLF exhibits several advantages compared with Nd:YAG including: reduced thermal lensing, a

polarized output, a long upper laser level lifetime and higher energy storage. Disadvantages include a lower thermal conductivity and less robust material. A side pumped design [29], produced a 7 W threshold and slope efficiency 0.506, TEM₀₀ mode.

Nd:YVO₄ has applications because of its high gain, emission cross section ≈ 5 times that of Nd:YAG. High gain is useful for some continuous applications, but amplified spontaneous emission militates against energy storage. Nd:YVO₄ output is polarized. Diode pumping a Nd:YVO₄ laser yielded 9 W in TEM₀₀ mode with a threshold of 2.5 W and a slope efficiency of 0.605, absorbed optical to optical [30].

Nd can be used to make efficient, high beam quality fiber lasers. A 12 μm core, Nd: fiber laser demonstrated: 9.2 W, a negligible threshold and 0.26 slope efficiency, launched optical to optical [31].

Tm:YAG produces laser wavelengths in the nominally eye safe region of the spectrum. Nominal eye safe wavelengths are wavelengths that are longer than about 1.4 μm . Long wavelengths are absorbed in the vitreous humor of the eye instead of being focused on the retina. Because the absorbing volume is much larger, the eye is relatively immune to laser induced damage. By codoping with Cr, a flash lamp pumped Tm:YAG laser, achieved a threshold of 43 J and a 0.045 slope efficiency [32]. With a lens duct coupling a laser diode array to a laser rod, a Tm:YAG laser achieved an output of 115 W in a highly multimode beam. Threshold was ≈ 40 W and slope efficiency was 0.36 [33]. Diode pumping from the side, a Tm:YLF laser demonstrated a threshold of 20 W with a slope efficiency of 0.37 [34]. Under pulsed operation, an end pumped configuration produced 300 mJ with a threshold of 460 mJ and slope efficiency of 0.29 [35].

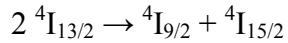
For flash lamp pumped operation, Ho:YAG is codoped with Tm, Er, and/or Cr. Absorption by Ho is weak in the visible. To achieve efficient operation, Cr and/or Er is used to provide strong absorption in the visible. Absorbed energy is then transferred to Tm and subsequently to Ho. Because Ho is a quasi 4 level laser, cooling is sometimes employed to decrease the

threshold. Despite the quasi 4 level nature, efficient flash lamp pumped laser operation was achieved with a threshold of 46 J and slope efficiency of 0.051 [36].

Diode pumped Ho lasers frequently use Tm codoping in YLF or an isomorph such as LuLF. Tm has an useful absorption band around 0.79 μm which is compatible with diode pumping. By promoting Tm self quenching and subsequent energy transfer to Ho, efficient operation can be achieved. There is a quasi equilibrium between the Tm ³F₄ and Ho ⁵I₇ manifolds [37]. Thus, not all stored energy can be extracted in a single Q-switched pulse. YLF is preferred over YAG because a deleterious energy transfer process where a Tm atom in the ³F₄ manifold interacts with a Ho atom in the ⁵I₇ manifold is much smaller. A side pumped design, achieved an optical to optical slope efficiency of 0.058 at room temperature in a single frequency, TEM₀₀ mode [38]. Threshold was 1.8 J and laser output energy was 110 mJ.

Yb:YAG lacks broad pump bands needed for flash lamp pumping but it excels with diode pumping. Diode pumping can use high performance InGaAs laser diodes in either an end pumped or a fiber design. Yb:YAG is a quasi 4 level laser but it has several advantages when compared to Nd:YAG. Advantages are: a longer lifetime, lower heat deposition, wider spectral bandwidth, and higher Yb concentrations. A single Yb:YAG thin disk laser produced 0.64 kW and multiple disks produced 1.0 kW [39]. Threshold was 185 W and slope efficiency was 0.60. A Yb: fiber laser produced 1.36 kW with a 40 W threshold and 0.83 slope efficiency, launched optical to optical [40].

Er:YAG and Er:YLF can produce many laser wavelengths Er:YAG, and its isomorphs, can operate in the 2.8 μm spectral region. Transitions are from the ⁴I_{11/2} to the ⁴I_{13/2} manifold. Because the ⁴I_{13/2} manifold is metastable, a population density can accumulate in it. Conversely, transitions at 1.66 μm occur between the ⁴I_{13/2} and ⁴I_{15/2} manifold. A large population density in the ⁴I_{13/2} manifold favors the second but militates against the first transition. Up conversion can occur where,



Because the $^4I_{9/2}$ manifold can quickly decay to the $^4I_{11/2}$ manifold, this process depletes 2 Er atoms from the $^4I_{13/2}$ manifold and creates 1 Er atom in the $^4I_{11/2}$ manifold. Thus, up conversion favors operation at 2.8 μm but does not favor operation at 1.66 μm . Selection of a laser material based on its up conversion energy transfer parameter becomes a consideration. At 2.69 μm , a flash lamp pumped Er:Tm:Cr:YAG achieved a threshold of 25 J and a slope efficiency of 0.006 [41]. A flash lamp pumped Er:Cr:YSGG laser achieved a threshold of ≈ 8 J and a slope efficiency of 0.01 [42].

Diode pumped Er lasers are possible both at 1.66 and 2.94 μm . For 2.69 μm operation, a high Er concentration, 0.50, end pumped Er:YAG disk had a 1.15 W output with a threshold of ≈ 0.25 W and slope efficiency of 0.34, absorbed optical to optical [43]. For 1.65 μm operation, a diode pumped Er:Yb:YAG produced 79 mJ using a 10 ms long pump pulse. Er and Yb concentrations were 0.01:0.05. Threshold was ≈ 2.0 J and the slope efficiency for the normal mode laser approached 0.034 [44].

If short wavelength flash lamp pumping is applied to Er:YLF, the $^4S_{3/2}$ manifold can produce 3 transitions. Transitions at 1.732 μm are to the $^4I_{9/2}$ manifold; at 1.231 μm to the $^4I_{11/2}$ manifold; and 0.850 μm to the $^4I_{13/2}$ manifold. A short pulse flash lamp in an Al cavity, yielded a threshold of 14 J and slope efficiency of 0.006 [45]. Single step diode pumping of the $^4S_{3/2}$ manifold is not presently done. However, 2 step laser diode pumping of this manifold is possible using a single pump wavelength. For example, a ≈ 0.8 μm photon can excite an Er atom to the $^4I_{9/2}$ manifold which can relax to the metastable $^4I_{13/2}$ manifold. A second pump photon raises the Er atom to the $^2H_{11/2}$ manifold which can relax to the $^4S_{3/2}$ manifold.

Cr:BeAl₂O₄ or alexandrite is a transition metal laser that can be tuned between ≈ 0.72 and 0.81 μm . Because there is a storage level in close proximity to the upper laser level, 4T_2 , the lifetime and emission cross section are highly temperature dependent. Also, there are 2 Cr sites, 1 with inversion symmetry and 1

with mirror symmetry complicating the spectroscopy. This material is operated at elevated temperatures often to take advantage of the increased emission cross section. A flash lamp pumped laser produced a threshold of 57 J and a slope efficiency of 0.052 [46]. Diode pumping can use the strong 4A_2 to 2E at 0.68 μm transition for pumping.

Ti:Al₂O₃ has a huge tuning range, stretching from 0.7 to >1.0 μm . Because of this tuning range, Ti:Al₂O₃ is often employed as a tunable laser source or for ultra short pulse generation. Ti:Al₂O₃ has a short upper laser level lifetime, about 3.2 μs at room temperature. This short lifetime makes flash lamp pumping difficult but possible. To circumvent this, Ti:Al₂O₃ is usually laser pumped, using a frequency doubled Nd:YAG laser. In this case, the Ti:Al₂O₃ output appears as a short, gain switched pulse, similar to a Q-switched pulse. The threshold depends on the resonator design and can be low. In turn, resonator design usually depends on the required laser output energy. A 180 mJ Ti:Al₂O₃ laser had a threshold of 190 mJ and slope efficiency of 0.53 [47]. Slope efficiency can approach the quantum defect, λ_p/λ_L .

Summary:

Solid state lasers are capable of storing energy which allows them to operate as optical integrators. This feature provides for Q-switched operation at a wide variety of pulse repetition frequencies and with good beam quality. Solid state laser efficiency is analyzed from a product of efficiencies point of view. Many of these efficiency factors are dependent on energy transfer processes which are characterized by energy transfer parameters. These parameters are often difficult to measure but they can be calculated. Laser performance of several solid state laser systems was characterized by a threshold and slope efficiency.

References:

1. T.H. Maiman, "Stimulated Optical Radiation In Ruby," *Nature* **187** 493-494 (1960)
2. J.C. Walling, O.G. Peterson, H.P. Jenssen, R.C. Morris, and E.W. O'Dell, "Tunable Alexandrite Lasers," *IEEE J. Quant. Elect.* **QE-16**, 1302-1314 (1980)

3. P.F. Moulton, "Spectroscopic And Laser Characteristics Of $Ti:Al_2O_3$," J. Opt. Soc. Am. B, **3** 125-133 (1986)
4. L.F. Johnson, H.J. Guggenheim, and R.A. Thomas, "Phonon Terminated Optical Masers," Phys. Rev., 179-185 (1966)
5. R.B. Allen and S.J. Scalise, "Continuous Operation Of A YAlG:Nd Diode Pumped Solid State Laser," Appl. Phys. Lett., 188-190 (1969)
6. N.P. Barnes, "Diode Pumped Solid State Lasers," J. Appl. Phys., 230-237 (1973)
7. C. J. Koester and E. Snitzer, "Amplification In A Fiber Laser," Appl. Opt. **3** 1182-1186 (1964)
8. R.J. Mears, L. Reekie, S.B. Poole, and D.N. Payne, "Neodymium Doped Silica Single Mode Fibre Lasers," Electronics Lett. **21** 738-740 (1985)
9. S. Yoshikawa, K. Iwamoto, and K. Washio, "Efficient Arc Lamps For Optical Pumping Of Neodymium Lasers," Appl. Opt. **10** 1620-1623 (1971)
10. J.P. Markiewicz and J.L. Emmett, "Design Of Flash Lamp Driving Circuits," IEEE J. Quant. Elect. **QE-2** 707-711 (1966)
11. C. Bowness, "On The Efficiency Of Single And Multiple Elliptical Laser Cavities," Appl. Opt. **4** 103-107 (1965)
12. J. Whittle and D.R. Skinner, "Transfer Efficiency Formula For Diffusely Reflecting Laser Pumping Cavities," Appl. Opt. **5** 1179-1182 (1966)
13. R.J. Beach, "Theory And Optimization Of Lens Ducts," Appl. Opt. **35** 2005-2015 (1996)
14. W.A. Clarkson and D.C. Hanna, "Two Mirror Beam Shaping Technique For High Power Diode Bars," Opt. Lett. **21** 375-377 (1996)
15. N.P. Barnes, M.E. Storm, P.L. Cross, and M.W. Skolaut Jr., "Efficiency of Nd Laser Materials With Laser Diode Pumping," IEEE J. Quant. Elect., **QE-26**, 558-569, (1990)
16. P.L. Cross, N.P. Barnes, M.W. Skolaut Jr., and M.E. Storm, "Blackbody Absorption Efficiencies For Six Lamp Pumped Nd Laser Materials," Appl. Opt., **29**, 791-797, (1990)
17. D.L. Dexter, "Theory Of Sensitizer Luminescence In Solids," J. Chem. Phys. **21**, 836-850 (1953)
18. T. Forester, "Experimentelle Und Theoretische Untersuchung Des Zwischenmerkularen Ubergangs Von Elektronenregungsenergie," Z. Naturf. **4A** 321-327 (1947)
19. N.P. Barnes, E.D. Filer, C.A. Morrison, and C.J. Lee, "Ho:Tm Lasers I: Theoretical," IEEE J. Quant. Elect. **QE-32** 92-103 (1996) and C.J. Lee, G. Han, and N.P. Barnes, "Ho:Tm Lasers II: Experiments," IEEE J. Quant. Elect. **QE-32** 104-111 (1996)
20. N.P. Barnes, W.J. Rodriguez, and B.M. Walsh, "Ho:Tm:YLF Laser Amplifier Performance," J. Opt. Soc. Am. B, **13** 2872-2882 (1992)
21. L.F. Johnson, J.E. Geusic, and L.G. Van Uitert, "Efficient, High Power, Coherent Emission From Ho^{3+} Ions In Yttrium Aluminum Garnet, Assisted By Energy Transfer," Appl. Phys. Lett. **8** 200-202 (1966)
22. N.P. Barnes and B.M. Walsh, "Amplified Spontaneous Emission – Application To Nd:YAG Lasers," IEEE J. Quant. Elect. **35** 101-109 (1999)
23. N.P. Barnes, K.E. Murray, and M. Jani, "Flash Lamp Pumped Ho:Tm:Cr:YAG And Ho:Tm:Er:YLF Lasers: Modeling Of A Single Long Pulse Length Comparison," Appl. Opt. **36** 3363-3374 (1997)
24. W.S. Martin and J.P. Chernoch, "Multiple internal Reflection Face Pumped Laser," U.S. Patent 3 633 126 (1972)
25. N.P. Barnes, D.J. Gettemy, L. Esterowitz, and R.E. Allen, "Comparison Of Nd 1.06 and 1.33 μm Operation In Various Hosts," IEEE J. Quant. Elect., **QE-23**, 1434-1451 (1987)
26. N.P. Barnes, B.M. Walsh, D.J. Reichle, and R.L. Hutcheson, "Nd:GYAG For Improved Performance At 0.946 μm ," Proceedings Of The Advanced Solid State Laser Conference, 108-110 (1998)
27. B.M. Walsh, N.P. Barnes, D.J. Reichle, R.L. Hutcheson, and R.W. Equall, "Compositional Tuning Of Nd:YAG To 0.94411 μm ," Proceedings Of The Advanced Solid State Laser Conference, 416-418 (1998)
28. S. Fujikawa, K. Furuta, and K. Yasui, "28% Electrical Efficiency Operation Of A Diode Side Pumped Nd:YAG Rod Laser," Opt. Lett. **26** 602-604 (2001)
29. K.J. Snell, D. Lee, K.F. Wall, and P. Moulton, "Diode Pumped, High Power CW And Mode Locked Nd:YLF Lasers," Proceedings Of Advanced Solid State Lasers TOPS **34** 55-59 (2000)

30. J. Ahang, M. Quade, K.M. Du, Y. Liao, S. Falter, M. Baumann, P. Loosen, and R. Poprawe, "Efficient TEM₀₀ operation Of Nd:YVO₄ Laser End Pumped By Fibre Coupled Diode Laser," Electron. Lett. **9** 775-777, (1997)
31. H. Zellmer, U. Willamowski, A. Timmermann, H. Welling, S. Unger, V. Reichel, H.R. Muller, J. Kirchhof, and P. Albers, "High Power CW Neodymium Doped Fiber Laser Operating At 9.2 W With High Beam Quality," Opt. Lett. **20** 578-580 (1995)
32. G.J. Quarles, A. Rosenbaum, C.L. Marquardt, and L. Esterowitz, "Efficient Room Temperature Operation Of A Flash Lamp Pumped Cr,Tm:YAG Laser At 2.01 μm ," Opt. Lett. **15** 42-44 (1990)
33. E.C. Honea, R.J. Beach, S.B. Sutton, J.A. Speth, S.C. Mitchell, J.A. Skidmore, M.A. Emanuel, and S.A. Payne, "115 W Tm:YAG CW Diode Pumped Solid State Laser," TOPS **10**, Advanced Solid State Lasers 307-309 (1997)
34. A. Dergachev, K. Wall, and P.F. Moulton, "A CW Side pumped Tm:YLF Laser," OSA TOPS **68** 343-346 (2000)
35. M. Petros, J. Yu, U.N. Singh, B.M. Walsh, N.P. Barnes, and J.C. Barnes, "A 300 mJ Diode Pumped 1.9 μm Tm:YLF Laser," Proceedings Of SPIE **4484** Lidar Remote Sensing For Industry And Environment Monitoring II, 17-24 (2002)
36. G.J. Quarles, A. Rosenbaum, C.L. Marquardt, and L. Esterowitz, "High Efficiency 2.09 μm Flashlamp Pumped Laser," Appl. Phys. Lett. **55** 1062-1064 (1989)
37. B.M. Walsh, N.P. Barnes, and B. DiBartolo, "On The Distribution Of Energy Between The Tm ³F₄ and Ho ⁵I₇ Manifold In Tm Sensitized Ho Luminescence," J. Of Luminescence, **75** 89-98 (1997)
38. J. Yu, U.N. Singh, N.P. Barnes, and M. Petros, "125 mJ, Diode Pumped, Injection Seeded, Ho:Tm:YLF Laser" Opt. Lett. **23** 780-782 (1998)
39. Chr. Stewen, M. Larionov, A. Giesen and K. Contag, "Yb:YAG Thin Disk Laser With 1.0 kW Output Power, Proceedings Of The Advanced Solid State Lasers Conference, TOPS Volume 34, 35-41 (2000)
40. J. Jeong, J.K. Sahu, D.N. Payne, and H. Nilsson, "Ytterbium Doped Large Core Fiber Laser With 1.36 kW Continuous Wave Output Power," Optics Express **12** 6088-6092 (2004)
41. R.K. Shori, A.A. Walston, O.M. Stafsudd, and M. Kokta, "Lasing Characteristics Of Free-Running And Q-switched, High Energy 2.69 μm Cr:Tm:Er:YAG Laser," Solid State Lasers XI, Proceedings Of SPIE **4630** (2002)
42. P.F. Moulton, J.G. Manni, and G.A. Rines, "Spectroscopic And Laser Characteristics Of Er:Cr:YSGG," IEEE J. Quant. Elect. **24** 960-973 (1988)
43. D.W. Chen, C.L. Fincher, T.S. Rose, F.L. Vernon, and R.A. Fields, "Diode Pumped 1 W Continuous Wave Er:YAG 3 μm Laser," Opt. Lett. **24** 385-387 (1999)
44. E. Georgiou, F. Kiriakidi, O. Musset, and J.P. Boquillon, "1.65 μm Er:Yb:YAG Diode Pumped Laser Delivering 80 mJ Pulse Energy," Optical Engineering **44** 064202-1-064202-10 (2005)
45. N.P. Barnes, R.E. Allen, L. Esterowitz, E.P. Chicklis, M.G. Knights, and H.P. Jenssen, "Operation Of A Er:YLF Laser At 1.73 Micrometers," IEEE J. Quant. Elect., **QE-22**, 397-343 (1986)
46. J.C. Walling, private communication
47. G.A. Rines and P.F. Moulton, "Performance Of Gain Switched Ti:Al₂O₃ Unstable Resonator Lasers," Proceedings On Advanced Solid State Lasers, **6** 88-93 (1990)

Resume: Education; PhD in Electrical Engineering, Masters in Physics, both from Ohio State University. Employment: Los Alamos National Laboratory and NASA Langley with sabbaticals at Naval Research Laboratory and University Of Southampton, UK Fellow of the Optical Society Of America and associate editor of IEEE Journal Of Electronics Publications: over 160 in refereed journals Presentations: over 180 at national or international conferences.

List of Figures

Figure 1. Transition metal atom showing bonding, 3d, and core electrons. Lanthanide series atom showing bonding, shielding, 4f, and core electrons.

Figure 2. Flash lamp and laser diode coupling schemes

Figure 3. Inverse lifetime of Nd:YAG and Nd:YLF versus Nd concentration

Figure 4. Normalized extraction efficiency versus number of times over threshold

Figure 5. Solid state laser geometries

Figure 6. Common lanthanide series laser transitions. Common laser diode pumps shown in 2 bands

Figure 7. Relaxation oscillations in Nd:YAG. 8 mJ laser output energy

List of Tables

Table 1. Sellmeier coefficients of common laser materials

Table 2. Spectroscopic properties of common laser materials

Table 3. Thermal and mechanical parameters of common laser materials

Table 2 Spectroscopic Parameters Of Common Laser Materials

Laser	Wave length	Life time	Upper level	Lower level	Z ₁	Z ₂	cross section	Line width
Nd:YAG	0.946	0.240	⁴ F _{3/2}	⁴ I _{9/2}	0.008	0.601	4.5	9.9
Nd:YAG	1.064	0.240	⁴ F _{3/2}	⁴ I _{11/2}	0.188	0.399	27.0	6.0
Nd:YAG	1.319	0.240	⁴ F _{3/2}	⁴ I _{13/2}	0.288	0.399	8.9	4.5
Nd:YLF π	1.047	0.520	⁴ F _{3/2}	⁴ I _{11/2}	0.261	0.430	21.4	13.8
Nd:YLF σ	1.053	0.520	⁴ F _{3/2}	⁴ I _{11/2}	0.261	0.570	13.7	12.4
Nd:YVO ₄ π	1.064	0.089	⁴ F _{3/2}	⁴ I _{11/2}	0.252	0.522	136.5	7.2
Nd:YVO ₄ σ	1.064	0.089	⁴ F _{3/2}	⁴ I _{11/2}	0.252	0.522	45.8	9.2
Ho:YAG	2.090	8.5	⁵ I ₇	⁵ I ₈	0.013	0.074	1.07	≈30
Ho:YAG	2.097	8.5	⁵ I ₇	⁵ I ₈	0.017	0.104	1.04	≈20
Ho:YAG	2.123	8.5	⁵ I ₇	⁵ I ₈	0.013	0.104	0.56	≈25
Ho:YLF π	2.052	14.0	⁵ I ₇	⁵ I ₈	0.025	0.087	1.49	14.1
Ho:YLF σ	2.063	14.0	⁵ I ₇	⁵ I ₈	0.029	0.087	0.99	13.5
Tm:YAG	2.01	10.5	³ F ₄	³ H ₆	0.018	0.455	0.22	5.5
Tm:YLF π	1.885	15.0	³ F ₄	³ H ₆	0.044	0.290	0.39	
Tm:YLF σ	1.907	15.0	³ F ₄	³ H ₆	0.032	0.290	0.25	
Er:YAG	1.645	6.9	⁴ I _{11/2}	⁴ I _{13/2}	0.022	0.215	0.45	≈20
Er:YAG	2.830	8.0	⁴ I _{13/2}	⁴ I _{15/2}	0.055	0.218	0.55	
Er:YLF	0.850	0.20	⁴ S _{3/2}	⁴ I _{13/2}	0.113	0.573		10
Er:YLF	1.231	0.20	⁴ S _{3/2}	⁴ I _{11/2}	0.159	0.573		
Er:YLF	1.732	0.20	⁴ S _{3/2}	⁴ I _{9/2}	0.107	0.573		
Yb:YAG	1.030	0.970	⁴ F _{5/2}	⁴ F _{7/2}	0.047	0.767	2.1	56
Nd:silica	1.060	0.460	⁴ I _{13/2}	⁴ I _{15/2}			1.3	320
Yb:silica	1.035	0.840	⁴ F _{5/2}	⁴ F _{7/2}			0.60	466
Cr:BeAl ₂ O ₄	0.72 -0.81	0.262	⁴ T ₂	⁴ A ₂			0.70	1410
Ti:Al ₂ O ₃	0.7- >1.0	0.003	² E	² T ₂			6.8	3720
Units	μm	ms					·10 ⁻²⁴ m ²	cm ⁻¹